S&G JOURNAL
ISSN: 1980-5160

DEVELOPMENT AND APPLICATION OF A NEW OFFSHORE WIND PROFILING METHODOLOGY

Luiz Felipe Rodrigues do Carmo
l.docarmo.meteoroufrj@gmail.com
Federal University of Rio de Janeiro (UFRJ), Rio de Janeiro, RJ, Brazil.

Ana Cristina Pinto de Almeida Palmeira
anapalmeira@igeo.ufrj.br
Federal University of Rio de Janeiro (UFRJ), Rio de Janeiro, RJ, Brazil.

Wellington Ceccopieri Belo
wceccopieri@petrobras.com.br
Leopoldo Américo Miguez de Mello Research, Development and Innovation Center - CENPES/ PETROBRAS, Rio de Janeiro, RJ, Brazil.

Luis Manoel Paiva Nunes
luismanoelpaiva@gmail.com
Federal University of Rio de Janeiro (UFRJ), Rio de Janeiro, RJ, Brazil.

ABSTRACT

Wind is an important variable to study because it is used for many purposes and, in extreme cases, causes natural disasters. From an energy point of view, it is a significant factor in wind power generation; therefore, its correct estimation is essential. Still, on this subject, estimating the vertical wind profile becomes essential since the wind turbines are not located on the surface but at higher levels. This study aimed to analyze offshore wind profiles using the estimation methodologies calculated in the work by Carmo *et al*. (2021) and compare them to a new methodology developed based on sea surface temperature (SST) and air temperature (T). To this end, data from the ERA5 Reanalysis, the P25 platform, and the buoy located on the P18 platform were used between August 1, 1999, and August 31, 1999. The findings showed that the method developed presented good results for the study region and that the atmosphere presented a neutral stability class, with Skill Score (SS) and Nash-Sutcliffe Efficiency (NSE) values that were relatively more representative than those of the other methods studied. Comparatively, the inclusion of TSM and T in the estimation of the profiles showed a significant improvement in the interpretation and accuracy of the results.

Keywords: Wind Profile; Energy; Temperature.

PROPPI / DOT
DOI: 10.20985/1980-5160.2023.v18n3.1911

INTRODUCTION

Brazil, a country located in South America, concentrates a large part of its border with the Atlantic Ocean, according to the 2017 Agro Census of the Brazilian Institute of Geography and Statistics (IBGE, 2017), approximately 10,900 km, or, percentage-wise, 39.2% of its maritime border. This is an issue to be highlighted since both the Brazilian coastal regions and the more distant offshore regions of the South Atlantic Ocean are important regions for the country from a social and economic perspective.

The increase in wind energy has been significant due to its size and favorable winds for energy exploitation. In the onshore region, wind energy is already a reality, with most of the wind farms located in the northeast of Brazil.

Specifically in the offshore region, as of 2019, with the imminent prospect of future offshore wind energy explorations in Brazil, the Brazilian Environment and Natural Resources Institute (IBAMA) held a workshop with various European experts and several Brazilian institutions to determine the environmental licensing rules for companies wishing to explore this region.

From that point onwards, the number of license applications has been steadily increasing, most of which are located off the coast of the states of Ceará, Rio Grande do Norte, Rio de Janeiro, and the southern region (IBAMA, 2022).

For these reasons, the knowledge and estimate of winds are increasingly essential for all maritime operations. Since platforms and wind farms have different structures and heights, it should be noted that wind estimates are relevant not only near the ocean surface but also at higher levels. More specifically, for wind energy, it is essential to know the wind profile at different atmospheric levels with great precision so that a wind farm is not installed in an unfavorable region or the wind turbine is not at a height that is not the most suitable. When this happens, losses can be incurred and profits minimized.

Atmospheric boundary layer

The transport processes on the Earth's surface at this boundary modify the lower levels of the atmosphere from 100 m to 3000 m, creating what is known as the Atmospheric Boundary Layer (ABL). Knowingly, the ABL can be defined as the part of the troposphere that suffers direct influence from the presence of the Earth's surface and responds to surface forcings on a timescale of around a few hours or less. These forces include frictional drag, evaporation and transpiration, heat transfer, pollutant emissions, and terrain-induced flow modification (Stull, 1988).

Classically, the atmospheric boundary layer can be subdivided into several sub-layers, such as the Convective Boundary Layer (CBL), the Surface Boundary Layer (SBL), the Residual Boundary Layer (RBL), the Stable or Nocturnal Boundary Layer (SBL or NBL), the Mixing Layer (ML), and the Entanglement Zone (EZ). More specifically, the SBL, the region of interest in wind energy studies, is the region at the bottom of the SBL where turbulent flows and stresses vary by less than 10% of their magnitude (Arya, 1981).

Throughout the oceans, the boundary layer depth varies relatively slowly in space and time. The sea surface temperature changes little over the diurnal cycle because of the tremendous mixing at the ocean top. In addition, water has a high heat capacity, which means it can absorb large amounts of heat from the sun with relatively little temperature change. Thus, a slow change in sea surface temperature means a slow change in the forcing to the bottom of the boundary layer (Stull, 1988).

Most changes in the depth of the boundary layer over the oceans are caused by synoptic and mesoscale processes of vertical movement and advection of different air masses over the sea surface. An air mass with a temperature different from the ocean will undergo a change as its temperature equilibrates with the sea surface. Once it is balanced, the depth of the resulting boundary layer can vary by only 10% over a horizontal distance of 1000 km. Exceptions to this smooth variation can occur near the boundaries between two ocean currents of different temperatures (Stage and Weller, 1986).

Another relevant factor is the presence of waves in the ocean, which further increases the complexity of estimating wind profiles. This is because the roughness varies and changes according to the wave's significant height and period. Therefore, considering the static roughness in the region (as is done in many parts of the continent) can also lead to significant errors (Donelan, 1990; Donelan *et al*., 1993; Carmo *et al*., 2021).

In the oceans, there is yet another complexity in the ABL region. Under the conditions of high values of significant wave height (Hs), the so-called Wave Boundary Layer (WBL) is formed. According to Chalikov and Babanin (2019), the Wave Boundary Layer (WBL) is defined as the lowest part of the ABL, where the fluctuations produced by the waves influence the atmospheric region just above. The WBL height can be calculated as a function of the significant wave height. **Equation 1** (Chalikov, 1986) is an example of how to calculate the estimated height of the

S&G Journal
Volume 18, Number 3, 2023, pp. 284-295
DOI: 10.20985/1980-5160.2023.v18n3.1911

WBL, established through the numerical modeling of movements produced by waves based on the two-dimensional Reynolds equations, in which ξ is the adjustment coefficient. Typical WBL heights can range from a few meters, in more extreme cases with high Hs, to almost 30 meters.

$$H_{CLO} = \xi_{aj} H_S \quad (1)$$

Near-shore ocean measurements and micrometeorological parameters

In the ocean, the most common form of measurement is *in situ* collection (mainly by meteoceanographic buoys) and remote sensors. Satellites are excellent alternatives and can be applied to various parameters other than winds, with the advantage of high spatial and temporal resolution. However, *in situ* data can provide greater accuracy in measurements.

With the scarcity of vertically measured data, it becomes necessary to estimate the wind profile of a given region using some alternative method or in alternative regions. However, the well-known methods for calculating profiles are not always suitable for direct application over the oceans and can often produce inaccurate results.

Given the scarcity of remote sensors, such as LIDARs, for example, for measuring wind at higher levels, it was necessary to investigate some alternative methods for determining these profiles. The most widely used and best known is the logarithmic wind profile method. Through the *in situ* measurements, it was observed that the wind profiles were approximately logarithmic, and therefore, it would be possible to determine an equation that represented this profile. Then, using the Pi-Buckingham theorem (Kantha and Clayson, 2000) and Monin and Obukhov's similarity theory (Monin and Obukhov, 1954; Wyngaard, 1973; Sorbjan, 1986; Stull, 1988), **Equation 2** is integrated, and **Equation 3** is obtained in the Surface Boundary Layer (SBL) to obtain the wind speed for a given height z:

$$\frac{kz}{u_*}\frac{\partial u}{\partial z} = \psi_M \quad (2)$$

$$u(z) = \frac{u_*}{k}\left[ln\left(\frac{z}{z_0}\right) - \psi_M\left(\frac{z}{L}\right)\right] \quad (3)$$

in which u is the wind speed, u_* is the friction speed, k is the Von-Karman constant, Zo is the roughness, and L is the Monin-Obukhov length.

In **Equation 3**, the term of the stability correction function is conventionally separated into three stability classes: stable, unstable, or neutral. It is crucial to properly establish the class to be used since, in non-neutral conditions, the buoyancy and heat flow parameters will be considered in the calculations of the equations.

Carmo *et al*. (2021) showed that, using the same methods for estimating friction velocity and roughness but with different stability classes, the wind profiles showed significant differences at higher levels of the atmosphere, and, consequently, the wind potential differed greatly in the neutral and stability scenarios. Therefore, the authors showed the importance of correctly calculating the stability correction term and, consequently, correctly estimating the Monin-Obukhov length (L).

In addition to the stability parameter and L, roughness (z_0) and friction velocity (u_*) are highly relevant in wind profile calculations. Roughness, in particular, has numerous solutions. For the offshore region, for example, the most widely used solutions are from Charnock (1955), Donelan (1990), Donelan *et al*. (1993), Chalikov (1995), and Taylor and Yelland (2001). In addition, Simiu and Scanlan (1978), Panofsky and Dutton (1984), Dyrbye and Hansen (1997), and JCSS (2001) also presented roughness values, or gamma (the power law term), for different surfaces, which greatly facilitated computational calculations (Carmo *et al*., 2021).

Some authors, such as Lange *et al*. (2004), showed that the roughness estimation models led to only small differences. He *et al*. (2019) found z_0 results with a systematic bias in the estimation models and proposed a change in the power exponent of z_0.

As Carmo *et al*. (2021) have shown, although some models show good results, research into wind profiles still needs to make great progress since the methods are still inefficient in many situations, and therefore, a more comprehensive method must be devised to improve the results and present wind and wind potential values closer to reality, minimizing losses.

With this in mind, this study aimed to estimate a new wind profile methodology, comparing it to the methodologies used in the work by Carmo *et al*. (2021) for the offshore region near the southeast coast of Brazil, here using ERA5 reanalysis data, the buoy located in the region of platform P18, and an anemometer located on platform P25.

METHODS AND DATA

Data

Data on Significant Wave Height (SWH), peak period (Tp), air temperature (T), sea surface temperature (SST), and wind

magnitude and direction were used from ERA5 reanalyses (with a spatial resolution of 0.25°x0.25° for meteorological data and 0.5°x0.5° for oceanographic data), buoy data located in the P18 platform region, and wind data located on the P25 platform for the period between August 1, 1999 and August 31, 1999, with a temporal resolution of 1 hour for ERA5. **Figure 1** shows the points studied.

Figure 1. Southeast Brazil study area with the P25 platform point and the meteoceanographic buoy located in the platform region (P18)

Methodology

Regarding the methodology used to calculate the wind profiles, the same methodologies were used as the profiles used, tested, and compared in the article by Carmo *et al*. (2021) (methodologies 1, 2, 3, and 4) and a new methodology (method 5) developed using T and TSM.

Initially, for all the methods, the Pi-Buckingham theorem (Kantha and Clayson, 2000) and Monin and Obukhov's similarity theory (Monin and Obukhov, 1954; Wyngaard, 1973; Sorbjan, 1986; Stull, 1988) will be used to determine them. As seen in the previous section, by integrating Equation 2, Equation 3 is obtained for wind speed at any height z in the region. Therefore, at first, the approximation for a neutral stability class profile () was considered, as proposed in the 2014 DNV-RP-C205 manual (**Equation 4**, adapted from **Equation 3**).

$$u(z) = \frac{u_*}{k}\left[ln\left(\frac{z}{z_0}\right)\right] \quad (4)$$

Later, stable average profiles will be considered since some regions may have this characteristic atmospheric regime, as was the case near the coast of Maranhão, as seen in the work by Carmo *et al*. (2021).

To clarify matters, each methodology applied to each simulated situation is described below.

Method 1: Typical z_0 values for different locations (DNV-RP-C205, 2014; Simiu and Scanlan, 1978; Panofsky and Dutton, 1984; Dyrbye and Hansen, 1997; JCSS, 2001)

In this method, the z_0 roughness values will be determined according to the ranges of maximum and minimum values found in the ocean regions. These values can be found in **Table 1** based on the DNV-RP-C205 manual (2014) for the values found by Simiu and Scanlan (1978), Panofsky and Dutton (1984), Dyrbye and Hansen (1997), and JCSS (2001).

Table 1. Roughness values and γ (adjustment constant used in the power law estimation method)

Terrain	z0 (m) minimum value	z0 (m) maximum value	
Windy coastal area	0.001	0.01	-
Open sea without waves	0.0001	0.0001	-
Open sea with waves	0.0001	0.01	0.12

These maximum (0.01) and minimum (0.0001) values were chosen because they fall within the ranges of the three classes in **Table 1** and also because these classes are the ones used in offshore studies, as follows: open sea without waves, open sea with waves, and coastal areas with onshore wind. This is essential since, with these extreme thresholds, it is possible to establish the maximum and minimum magnitude of the wind at a given level for any type of situation, considering a neutral atmosphere.

The friction velocity term was calculated from the average wind speed at a given height H (u_H) above the sea surface (indirect method). Thus, u_* was obtained from **Equation 5**, in which ω is taken to be the surface friction coefficient (surface drag coefficient), defined by **Equation 6**, and β is the logarithm of the height by the squared roughness.

$$u_* = \sqrt{\omega}\, u_H \quad (5)$$

$$\omega = \frac{k^2}{\beta^2} \quad (6)$$

With **Equations 5** and **6** solved and considering the minimum and maximum roughness established, the maximum and minimum wind speeds for a height z are calculated using **Equations 7** and **8** (adapted from **Equation 4**), in this case considering a neutral atmosphere.

S&G Journal
Volume 18, Number 3, 2023, pp. 284-295
DOI: 10.20985/1980-5160.2023.v18n3.1911

$$u_{min}(z) = \frac{u_*}{k}\left[ln\left(\frac{z}{z_{0\,min}}\right)\right] \quad (7)$$

$$u_{max}(z) = \frac{u_*}{k}\left[ln\left(\frac{z}{z_{0\,max}}\right)\right] \quad (8)$$

Method 2 – Wind profile calculated from z_0 from Donelan (1990)

In this method, the roughness value was calculated using the method of Donelan (1990), who obtained, through field experiments, z_0 values from a direct function of the significant wave height given by **Equation 9**.

$$z_{0\,Don90} = \xi\left(\frac{H_s}{4}\right) \quad (9)$$

where: Hs is the significant wave height and ξ is constant.

Using **Equations 5** and **6** again to determine the friction velocity, the wind speed for a height z is obtained from **Equation 10** for a neutral atmosphere.

$$u(z) = \frac{u_*}{k}\left[ln\left(\frac{z}{z_{0\,Don90}}\right)\right] \quad (10)$$

Method 3 - Wind profile calculated from z_0 from Donelan *et al.* (1993)

Donelan *et al*. (1993) determined a relationship between roughness and the wave age parameter term through experiments and numerical tests. The representation of these terms is essential because they influence the sea state in the Wave Boundary Layer (WBL). Therefore, **Equation 11** contains the solution used to calculate roughness.

$$z_{0\,Don93} = \varphi\left(\frac{H_s}{4}\right)\left(\frac{u_{10}}{c_p}\right)^{\mu} \quad (11)$$

Equations 7 and **8** are used again to determine the friction velocity, so the wind speed for a height z is obtained from **Equation 12** for a neutral atmosphere.

$$u(z) = \frac{u_*}{k}\left[ln\left(\frac{z}{z_{0\,Don93}}\right)\right] \quad (12)$$

Method 4 - Wind profile calculated from z_0 of Taylor and Yelland (2001) for different classes of atmospheric stability

Since Taylor and Yelland's (2001) method is the main method for estimating ocean roughness and has been used constantly, with various applications in corrections and changes to its adjustment parameters, it will also be applied in this study. In addition, the calculation of the stability classes of the atmosphere will now also include unstable, neutral, and stable. Therefore, the L term will need to be calculated. To this end, they were calculated using the relationships and solutions of Businger *et al*. (1971), Dyer (1974), Nickerson and Smiley (1975), Benoit (1977), Arya (1988), Hansen *et al*. (2012), and Carmo *et al*. (2021).

Equation 13, which represents the Taylor and Yelland (2001) method, was thus used. As previously mentioned, this method generally leads to the best results because it uses significant wave height (Hs) and peak period (Tp) in its calculations. Therefore, z_0 will represent a large part of the processes involved in this region.

$$z_{0\,TY01} = \mu H_s\left(\frac{H_s}{L_p}\right)^{\alpha}, \quad and \quad L_p = \left(\frac{gT_p^2}{2\pi}\right) \quad (13)$$

Again using **Equations 7** and **8** to determine the friction velocity, the wind speed for a height z is obtained from **Equations 14 (stable atmosphere)**, **15 (neutral atmosphere)**, and **16 (unstable atmosphere)**, where ζ is a function of z/L.

$$u(z) = \frac{u_*}{k}\left[ln\left(\frac{z}{z_{0\,TY\,01}}\right) + \psi_M(\zeta)_{EST}\right] \quad (14)$$

$$u(z) = \frac{u_*}{k}\left[ln\left(\frac{z}{z_{0\,TY\,01}}\right)\right] \quad (15)$$

$$u(z) = \frac{u_*}{k}\left[ln\left(\frac{z}{z_{0\,TY\,01}}\right) - \psi_M(\zeta)_{INS}\right] \quad (16)$$

Method 5 - New method developed - Calculation of z_0 and as a function of T, TSM, Hs, and Tp

Aiming to further increase the accuracy of the results for wind profiles, this work will develop a new method that will be adapted from the methods of Taylor and Yelland (2001) and Carmo *et al*. (2021) for roughness. This method will be innovative, as in addition to using the Hs and Tp variables already included in Taylor and Yelland (2001) and Carmo *et al*. (2021), it will also use the air temperature (T) and sea surface temperature (SST) variables. This was an important step, as inserting T and TSM will indirectly represent the heat flow in the region and give a better idea of its direction and intensity. **Figure 2** shows an example of this process.

S&G Journal
Volume 18, Number 3, 2023, pp. 284-295
DOI: 10.20985/1980-5160.2023.v18n3.1911

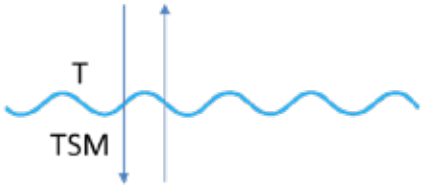

Figure 2. Representation of the interaction between air temperature (T) and sea surface temperature (SST)

More clearly, in this new method, the adjustment parameters of the Taylor and Yelland (2001) roughness method will be calculated empirically due to the ratio of T and TSM, obtaining more representative values for the region of interest. New correction parameters will be used for the Monin-Obukhov length and, thus, for the Richardson number to calculate the instability parameter. Repeating **Equations 7** and **8** to determine the friction velocity leads to **Equations 17** and **18** for roughness and profile.

$$z_0' = \vartheta'(T, TSM) H_s \left(\frac{H_s}{L_p}\right)^{\gamma(T,TSM)}, \; and \quad L_p = \left(\frac{gT_p^2}{2\pi}\right) \quad (17)$$

$$u(z) = \frac{u_*}{k}\left[ln\left(\frac{z}{z_0'}\right) + \psi'_M\left(\zeta'_{[z,L(T,TSM)]}\right)\right] \quad (18)$$

RESULTS

Figure 3 shows the average wave boundary layer (WBL) for the period studied in the region of the points of interest. It can be seen that, in this case, the WBL does not exceed 10 meters. Therefore, disregarding it (only in this specific situation) will not cause major problems in estimating the wind profiles because the profiles are estimated by considering the wind at 10 meters. In cases where its height exceeds this value, it is necessary to consider it and, consequently, re-evaluate the methodology for estimating the profiles, including the height of the parameterized WBL.

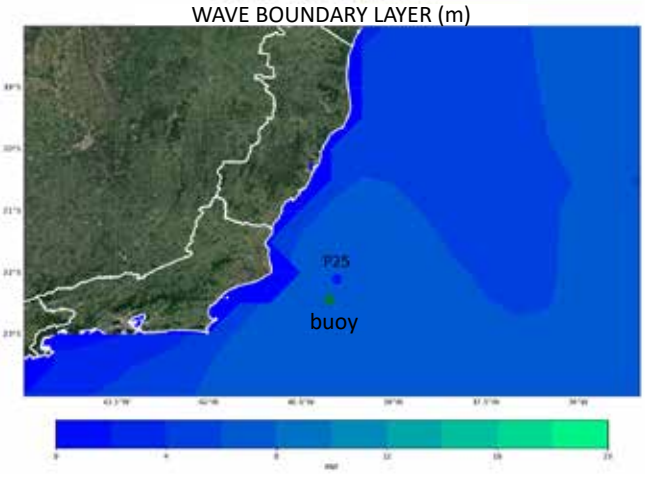

Figure 3. Average Wave Boundary Layer Height (WBL) for August 1999

Figures 4a, **4b**, and **4c** show the wind roses (with wind direction and magnitude) from the ERA5 reanalysis for the buoy point located on platform P18 and for platform P25. A qualitative comparison of the ERA5 results (**Figure 4a**) with the P18 buoy (**Figure 4b**) shows little difference in wind direction, except in the southeast quadrant (between 90° and 135°), where there was a slight difference in direction. In terms of magnitude, the highest values were recorded at buoy P18. When comparing the data from the P25 platform (**Figure 4c**) to the data from the P18 buoy (**Figure 4b**), no significant variation in wind direction could be observed either. In this case, this may be a significant consideration as the wind direction may not be varying significantly with height. Therefore, this could indicate that the average atmospheric profile of the region should be neutral. This will be confirmed or not in the wind profile figures below.

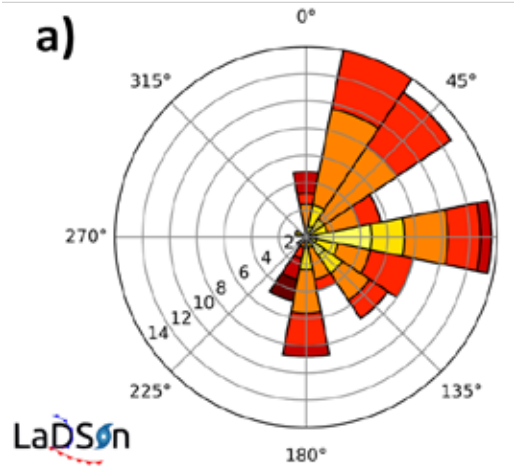

S&G Journal
Volume 18, Number 3, 2023, pp. 284-295
DOI: 10.20985/1980-5160.2023.v18n3.1911

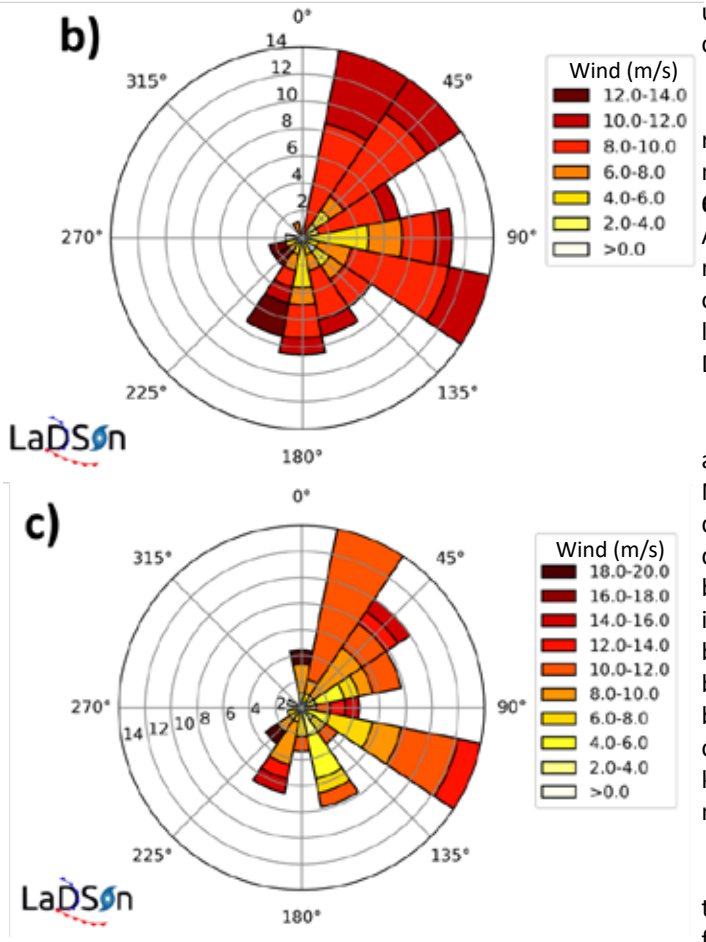

Figure 4. Wind rose from the ERA5 reanalysis (a) for buoy P18 (b) and platform P25 (c) for August 1999.

Figure 5 shows the comparison and difference between the significant wave height of ERA5 and that of the buoy located in the P18 platform region. It can be seen that the ERA5 showed more significant differences compared to the buoy at the higher Hs values. These differences are often expected since some studies, such as that by Carmo *et al*. (2020), show that it is precisely in the extreme values that the ERA5 reanalysis ends up differing from the observed Hs values. This further highlights the importance of using meteorological buoys to estimate profiles since some methods use significant height as input data. Therefore, using ERA5 can further contribute to error propagation.

Figures 6, **7**, **8**, and **9** show the comparison and difference between the wind magnitude estimated by the DNV method, the new method developed for buoy P18 (**Figures 6** and **7**), and the data on platform P25 (**Figures 8** and **9**). A qualitative comparison of the figures shows that the two methods underestimate the wind values compared to the observed data from the buoy and the platform. Nevertheless, the developed method seems more assertive than the DNV method.

This greater assertiveness can be confirmed in **Tables 2** and **3**, showing that the model had better results for BIAS, NSE, and SS. The correlations were similar, and the method developed had a slight increase in standard deviation, which does not influence its performance since this difference (in both cases) does not exceed 0.3. Another notable factor is that, in the study by Carmo *et al*. (2021), this difference between the DNV method and the new methods suggested by them was bigger, and the model performed even better because, in the region studied by the authors, the region's characteristic atmospheric regime proved to be stable (unlike the P18 and P25 regions that showed a characteristically neutral regime, closer to the methods proposed by DNV).

Figure 10 shows the average profiles for August 1999, estimated by each method. This figure shows some relevant factors. Although the Donelan (1990) and Donelan *et al*. (1993) methods are very close (on average) to the values observed on the P25 platform, it is noted that the curve of the wind profiles of these methods is very different from what would be considered "ideal." In other words, on the surface, the estimated values are very far from the values observed at the buoy located at P18. However, in the method developed, the values are close at both P18 and P25, confirming that the profile is closer to that characteristic of the region. This result is highly relevant and confirms what was shown in the previous tables, as it reveals that the insertion of temperature and TSM helped adjust the profiles to present more accurate results.

S&G Journal
Volume 18, Number 3, 2023, pp. 284-295
DOI: 10.20985/1980-5160.2023.v18n3.1911

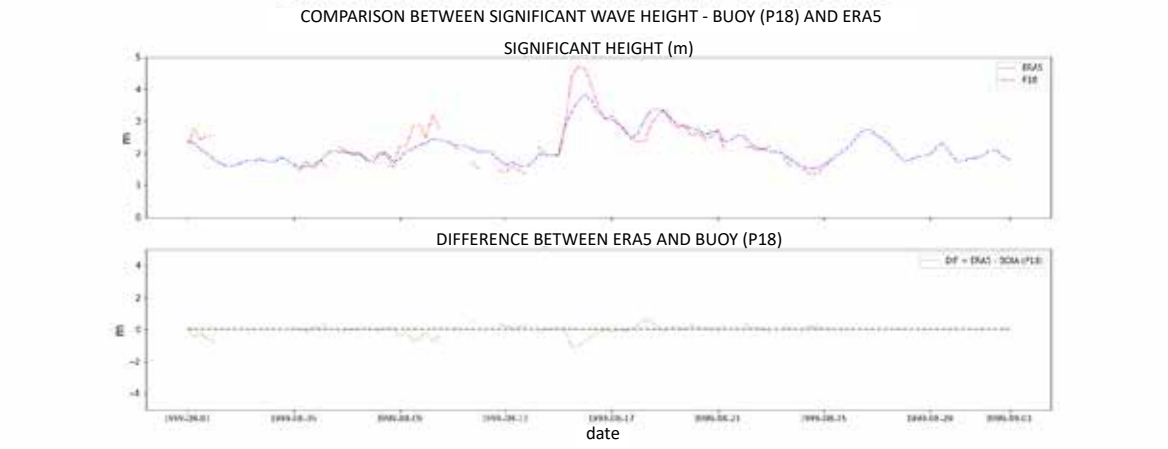

Figure 5. Significant wave height of the buoy (P18) and ERA5 and the difference between the significant wave heights of the two

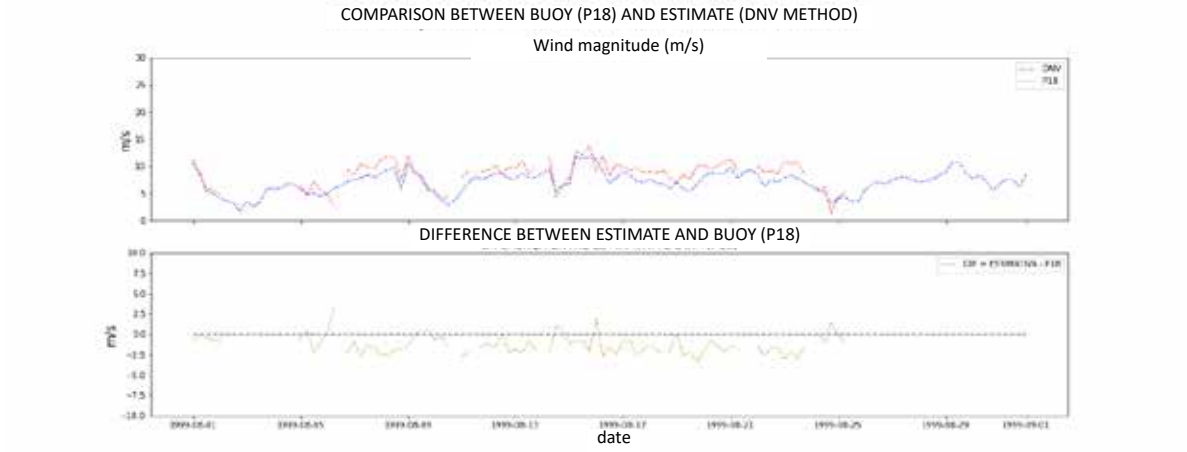

Figure 6. The wind magnitude estimated by the DNV method and the buoy wind (P18) and the difference in significant heights between the two.

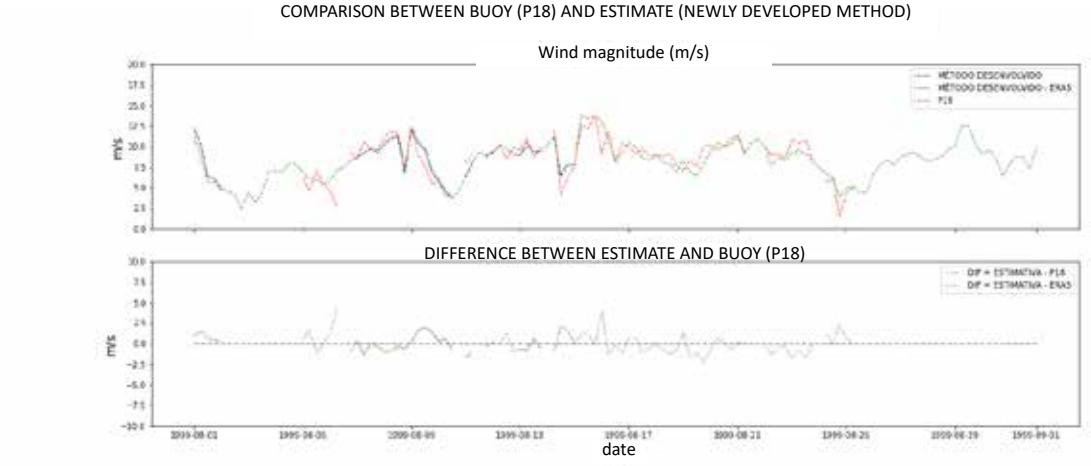

Figure 7. Wind magnitude estimated by the new method developed and the buoy wind (P18) and the difference in significant heights between the two.

S&G Journal
Volume 18, Number 3, 2023, pp. 284-295
DOI: 10.20985/1980-5160.2023.v18n3.1911

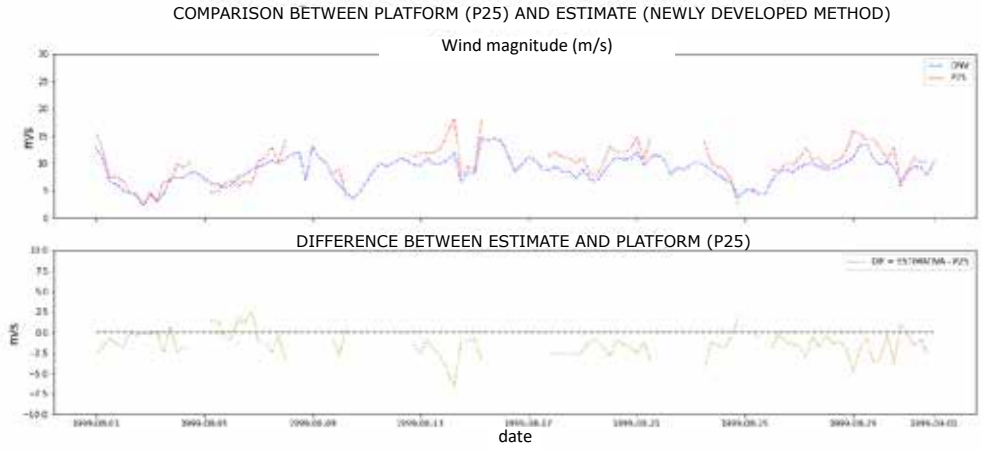

Figure 8. Wind magnitude estimated by the DNV method and the wind of the platform (P25) and the difference in significant heights between the two.

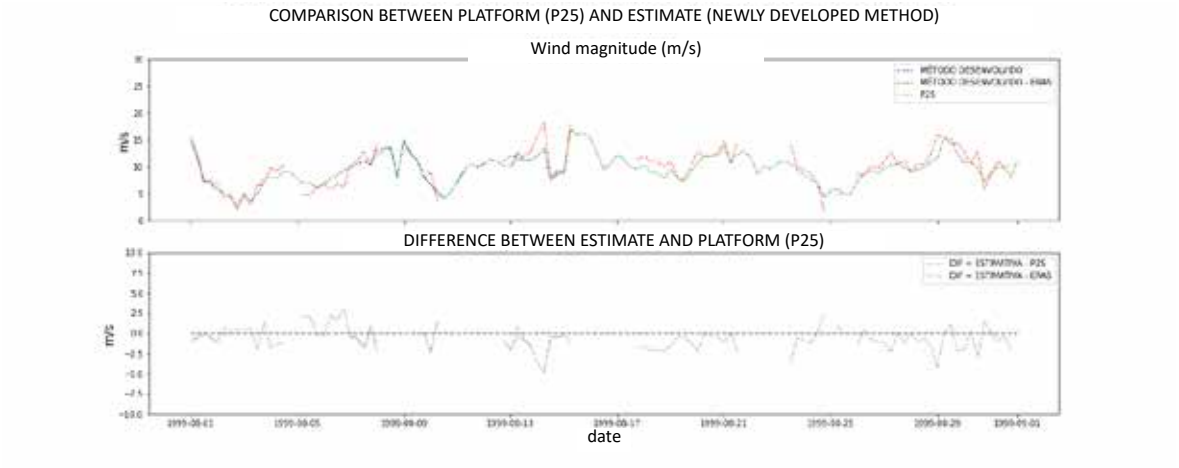

Figure 9. The wind magnitude estimated by the method developed, the wind from the P25 platform, and the difference in significant heights between the two.

Finally, **Figures 11** and **12** show examples of average roughness estimates using the Donelan (1990) method and the method developed for the period of August 1999. It is noted that, with the TSM and T insertion (in the new method), the calculated roughness shows variations in this parameter in locations that did not appear in the Donelan (1990) method, for example. In other words, this method could be more assertive if used in other locations. Furthermore, using a tabulated roughness value, i.e., without varying its value in space and time, can lead to even greater errors, which were shown, for instance, in this study and in the studies by Carmo *et al*. (2021) and He *et al*. (2019).

S&G Journal
Volume 18, Number 3, 2023, pp. 284-295
DOI: 10.20985/1980-5160.2023.v18n3.1911

Table 2. Comparison between the statistical metrics calculated for the P18 point

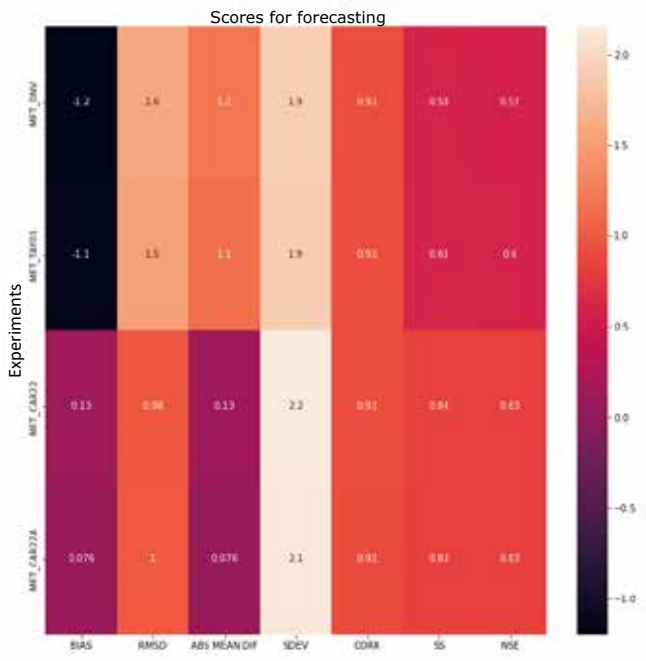

Table 3. Comparison between the statistical metrics calculated for the P25 point

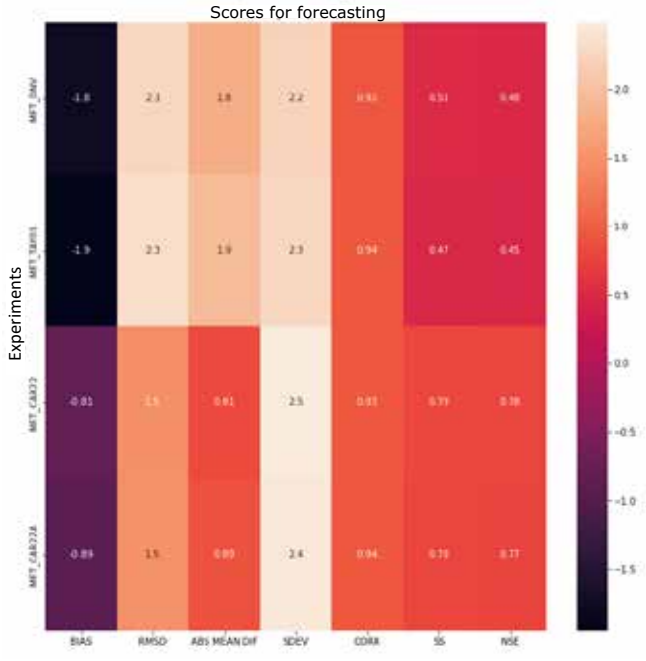

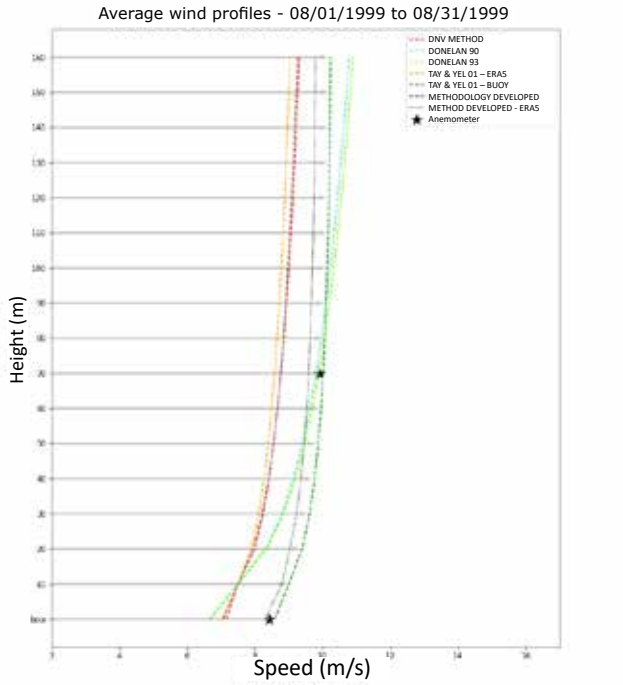

Figure 10. Estimated wind profiles for the DNV methods Donelan (1990), Donelan *et al*. (1993), Taylor and Yelland (2001), adapted by Carmo *et al*. (2021), and the developed method

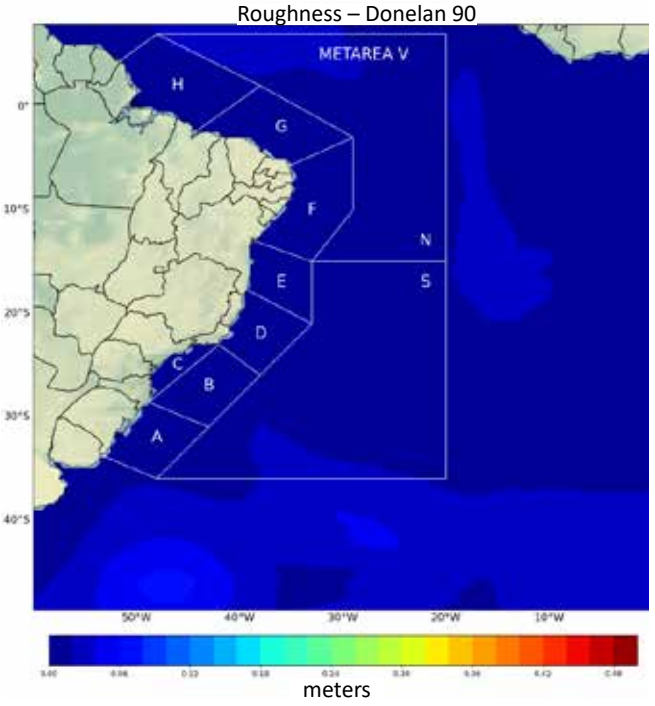

Figure 11. Roughness calculated using the Donelan 90 method for the period of August 1999.

S&G Journal
Volume 18, Number 3, 2023, pp. 284-295
DOI: 10.20985/1980-5160.2023.v18n3.1911

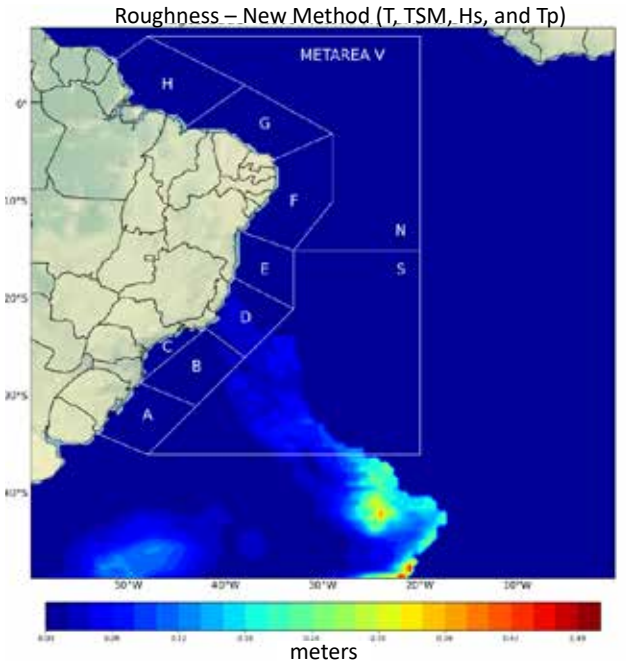

Figure 12. Roughness calculated using the new method developed for the period of August 1999.

CONCLUSIONS

Among the conclusions, it can be emphasized that new methodologies for estimating wind profiles are welcome and that the subject has not yet been exhausted. With regard to roughness, it was found that different methods produced significantly different results. Therefore, for the region of interest in each study, each of these methods should be tested to see which gives the best results.

In the work by Carmo *et al*. (2021), for example, the Taylor and Yelland method proved to be more satisfactory than others, such as Donelan (1990) and Donelan *et al*. (1993). In this study, the Taylor and Yelland (2001) roughness method adapted to T and TSM showed even more satisfactory results, revealing that there is still progress to be made.

Lange *et al*. (2004) showed in their study that the models for estimating roughness led to only small differences. However, this study showed that this difference completely altered the results.

As for the stability correction parameter, this study concluded that it must be calculated regardless of whether the region is neutral, stable, or unstable. Carmo *et al*. (2021) found that the region of interest in their study was stable and thus ended up significantly modifying the results. Although the region studied is classically neutral, adopting a stability value of zero is not ideal as the value is not zero but close to zero. This will produce errors in the profile estimates and change the logarithmic profile of the estimated winds. These errors will significantly impact other relevant calculations, such as wind potential studies (since the potential is a function of the cubed wind).

In this vein, it can also be concluded that when there are concomitant errors between roughness and stability determination, the problem is even more significant. Therefore, great care must be taken when estimating these profiles in the ocean since they have "live" roughness. This means that it is directly affected by the significant wave heights in the region and is not a fixed, static value, as already mentioned. Adding to the complexity, the higher the values of significant wave height, the greater the height of the Wave Boundary Layer (WBL). This implies a change in the paradigms for estimating wind profiles because within the WBL, winds will behave differently from those estimated for the Surface Boundary Layer.

In summary, this work shows the importance of calculating the micrometeorological parameters correctly for your region and the significance of determining their stability class. Without these, the models' results may show an erroneous estimate and produce inadequate studies that will not represent the reality of the region of interest.

REFERENCES

Arya, P.S. (1981), "Parameterizing the height of the stable atmospheric boundary layer", *Journal of Applied Meteorology*, Vol. 20, pp. 1192-1202.

Arya, P.S. (1988), *Introduction to Micrometeorology*, 2nd ed., Academic Press, San Diego.

Benoit, R. (1977), "On the integral of the surface layer profile-gradient functions", *Journal of Applied Meteorology and Climatology*, Vol. 16, No. 8, pp. 859–860.

Businger, J.A., Wyngaard, J.C., Izumi, Y., Bradley, E.F. (1971), «Flux profile relationships in the atmospheric surface layer", *Journal of the Atmospheric Sciences*, Vol. 28, pp. 181-189.

Carmo, L.F.R., Palmeira, A.C.P.A., Antonio, C.F.J.L. (2020), "Estimativa do perfil de vento e potencial eólico offshore para costa de Cabo Frio", *Revista Sistemas & Gestão*, Vol. 15, No. 1, pp. 46-52.

Carmo, L.F.R., Palmeira, A.C.P.A., Antonio, C.F.J.L., Palmeira, R.M.J. (2021), "Comparison of wind profile estimation methods for calculating offshore wind potential for the Northeast region of Brazil", *International Journal of Energy and Environmental Engineering*, Vol. 13, pp. 365-375.

Chalikov, D., Babanin, A.V. (2019), "Parameterization of wave boundary layer", *Atmosphere*, Vol. 10, p. 686.

Chalikov, D.V. (1995), "The parametrization of the wave boudary layer", *Journal of Physical Oceanography*, Vol. 25, pp. 1333–1349.

Charnock, H. (1995), "Wind stress on a water surface", *Quarterly Journal of the Royal Meteorological Society*, Vol. 81, pp. 639-640.

DNV (2014), *Reccommended Practice - DNV-RP-C205 on Environmental Conditions and Environmental Loads*, DNV, disponível em: www.dnv.com

Donelan, M.A. (1990), *Air-Sea interaction, from the sea: ocean engineering science*, Vol. 9 (two volume set), John Wiley & Sons.

Donelan, M.A., Dobson, F.W., Smith, S.D., Anderson, R.J. (1993), "On the dependence of sea surface roughness on wave development", *Journal of Physical Oceanography*, Vol. 23, pp. 2143–2149.

Dyer, A.J. (1974), "A review of flux-profile relations", *Boundary-Layer Meteorology*, Vol. 1, pp. 363-372.

Dyrbye, C., Hansen, S.O. (1997), *Wind loads on structures*, John Wiley & Sons, Chichester, England.

Hansen, K.S., Barthelmie, R.J., Jensen, L.E., Sommer, A. (2012), "The impact of turbulence intensity and atmospheric stability on power deficits due to wind turbine wakes at Horns Rev wind farm", *Journal of Wind Engineering and Industrial Aerodynamics*, Vol. 15, No. 1.

He, Y.C., Fu J.Y., Shu Z.R., Chan P.W., Wua J.R., Li Q.S. (2019), "A comparison of micrometeorological methods for marine roughness estimation at a coastal area", *Journal of Wind Engineering & Industrial Aerodynamics*, pp. 195-104010.

IBAMA - Instituto Brasileiro do Meio Ambiente e dos Recursos Naturais Renováveis (2022), *Licenciamento ambiental federal*, IBAMA, disponível em: http://www.ibama.gov.br/laf/consultas/mapas-de-projetos-em-licenciamento-complexos--eolicos-offshore (acesso em: 17 nov. 2022)

JCSS - Joint Committee on Structural Safety (2001), *JCSS Probabilistic Model Code Part 2*: *load models*.

Kantha, L.H., Clayson, C.A. (2000), *Small scale processes in geophysical fluid flows*, Academic Press, San Diego, 883 p.

Lange, B., Larsen, S., Højstrup, J., Barthelmie, R. (2004), "Importance of thermal effects and sea surface roughness for offshore wind resource assessment", *Journal of Wind Engineering & Industrial Aerodynamics*, Vol. 92, No. 11, pp. 959-988.

Monin, A.S., Obukhov, A.M. (1954), "Basic Laws of turbulent mixing in the atmosphere near the ground", *Trudy Instituta Geologiceskogo Akademii Nauk SSSR*, Vol. 24, No. 151.

Nickerson, E.C., Smiley, V.E. (1975), "Surface layer and energy budget parametrizations for mesoscale models", *Journal of Applied Meteorology*, Vol. 14, pp. 297-300.

Panofsky, H.A., Dutton, J.A. (1984), *Atmospheric turbulence, models and methods for engineering applications*, John Wiley & Sons, New York, NY.

Simiu, E., Scanlan, R.U. (1978), *Wind effects on structures: an introduction to wind engineering*, John Wiley & Sons, New York, NY.

Sorbjan, Z. (1986), "On similarity in the atmospheric boundary layer", *Boundary-Layer Meteorology*, Vol. 43, pp. 377-397.

Stage, S.A., Weller, R.A. (1986), "The frontal air-sea interaction experimente (FASINEX) part II: experimental plan", *Bulletin of the American Meteorological Society*, Vol. 67, pp. 16-20.

Stull, R.B. (1988), *An introduction to boundary layer meteorology*, Kluwer Academic Publishers, Dordrecht, Netherlands, 667 p.

Taylor, P.K., Yelland, M.J., (2001), "The dependence of sea surface roughness on the height and steepness of the waves", *Journal of Physical Oceanography*, Vol. 31, No. 2, pp. 572–590.

Wyngaard, J.C. (1973), "On surface layer turbulence", in Haugen, D.A. (ed.), *Workshop on micrometeorology*, American Meteorological Society, Boston, MA, pp. 101-148.

Received: December 1, 2022

Approved: December 4, 2023

DOI: 10.20985/1980-5160.2023.v18n3.1911

How to cite: Carmo, L.F.R., Palmeira, A.C.P.A., Belo, W.C., Nunes, L.M.P. (2023). Development and application of a new offshore wind profiling methodology. Revista S&G 18, 3. https://revistasg.emnuvens.com.br/sg/article/view/1911